

1
2
3 Establishment and characterization of a squamous cell carcinoma cell line, designated
4 hZK-1, derived from a metastatic lymph node tumor of the tongue
5
6

7 Tetsuya Hirabayashi, Haruka Takahashi, Miho Watanabe, Toshiaki Tachibana (✉)
8
9

10 T. Hirabayashi

11
12 Department of Anatomy, The Jikei University School of Medicine, 3-25-8
13 Nishishinbashi, Minato-ku, Tokyo, 105-8461, Japan;
14

15
16 H. Takahashi, M. Watanabe

17
18 Department of Oral & Maxillofacial Surgery, Nippon Dental University School of Life
19 Dentistry at Niigata, 1-8 Hamaura-cho, Chuo-ku, Niigata 951-1500, Japan
20

21 Department of NDU Life Sciences, School of Life Dentistry, The Nippon Dental
22 University, 1-9-20 Fujimi, Chiyoda-ku, Tokyo, 102-8159, Japan
23
24

25
26 T. Tachibana (✉)

27
28 Division of Fine Morphology, Core Research Facilities, The Jikei University School of
29 Medicine, 3-25-8, Nishi-Shinbashi, Minato-ku, Tokyo, 105-0082, Japan
30

31 Tel: +81-3-3433-1111 ex, 2431

32
33 e-mail: t-tachibana@jikei.ac.jp
34
35

36 Summary

37 The hZK-1 cell line was successfully established from the metastatic foci of a lymph
38 node of an 82-year-old Japanese woman with squamous cell carcinoma of the tongue.
39 The pathological diagnosis of the tumor was moderately to well-differentiated
40 squamous cell carcinoma. The hZK-1 cells were angular in shape, and had neoplastic
41 and pleomorphic features. Adjacent hZK-1 cells were joined by desmosomes and well
42 developed microvilli, and many free ribosomes were observed in the cytoplasm. The
43 doubling time of the hZK-1 cells was approximately 36, 33, and 29 h at the 10th, 20th and
44 30th passage, respectively. The cell line was shown to be triploid, with a chromosomal
45 distribution of 75 to 80. Immunocytochemical staining of the hZK-1 cells revealed
46 cytokeratin (CK) 17-, Ki67- and p53-positive staining, and negative staining for CK13.
47 The hZK-1 cells were negative for human papillomavirus (HPV)-16 or-18 infection.
48 Grafting was not successful when the hZK-1 cells were transplanted into the subcutis of
49 SCID mice. The hZK-1 cells (2×10^6 cells/3 ml of growth medium) secreted vascular
50 endothelial growth factor (VEGF) that reached a concentration of 2.6 ng/ml media after
51
52
53
54
55
56
57
58
59
60
61
62
63
64
65

1
2
3 3 days of culture. Hypoxia enhanced cellular HIF-1 α expression and VEGF secretion in
4 hZK-1 cells. The HIF-1 α inhibitor YC-1 partially inhibited hypoxia-induced VEGF
5 secretion in ZK-1 cells. The reverse transcription-polymerase chain reaction (RT-PCR)
6 results revealed that the expression of CK17, Ki67 and p53 was elevated in the hZK-1
7 cells. hZK-1 cells were not sensitive to CDDP, TXT, 5-FU, or a mixture of these 3
8 anti-tumor agents.
9
10
11
12

13 Introduction

14 Oral squamous cell carcinoma (OSCC) is the most prevalent malignant tumor in the
15 head and neck region, comprising more than 90% of all oral malignancies¹. With the
16 exception of distant metastases, nearly 50% of patients with OSCC present with clinical
17 or pathological evidence of lymph node metastasis². In addition, there are reports of
18 metastasis to lung or bone³. There are several squamous cell carcinoma cell lines
19 derived from tongue^{4, 5, 6, 7, 8}. Patient's with lingual carcinoma are associated with
20 excessive alcohol consumption, history of tobacco use, and human papillomavirus (HPV)
21 infection⁹.
22
23
24
25
26
27

28 Vascular endothelial growth factor (VEGF) is a major regulator of angiogenesis^{10,11}. It
29 has been reported that various kinds of cancer cells produce VEGF. VEGF induces
30 endothelial cell proliferation, migration and the formation of blood vessels^{12,13}.
31 Hypoxia-inducible factor-1 (HIF-1) plays a critical role in angiogenesis by activating the
32 transcription of genes that encode pro-angiogenic growth factors, including VEGF¹⁴.
33 HIF-1 α is an oxygen-sensitive subunit of HIF-1 and its expression is rapidly increased
34 under hypoxic conditions¹⁵.
35
36
37
38

39 We report herein the establishment and characterization of a new cell line, designated
40 hZK-1, which was derived from a metastatic lymph node in squamous cell carcinoma of
41 the tongue. Since it has been reported that 18-36% of cell lines contain a misidentified
42 species or cell type¹⁶, and that 18% of cell lines donated to the German Cell Bank were
43 misidentified or contaminated¹⁷, we checked cross-contamination of these hZK-1 cells
44 with Nialym cells that we had previously established from tongue cancer⁸. The hZK-1
45 cell line may provide valuable information on the biological properties and therapeutic
46 responses of specific cancer types, and may lead to the development of effective
47 treatments.
48
49
50
51
52
53

54 Materials and Methods

55
56
57
58
59
60
61
62
63
64
65

Medical history

The patient was an 82-year-old Japanese woman. The histopathological diagnosis was moderately to well-differentiated squamous cell carcinoma of the tongue. She received TPF therapy, which is a combination of 150 mg of taxotere (TXT), 150 mg of cisplatin (CDDP) and 5000 mg of 5-fluorouracil (5-FU), as preoperative chemotherapy. Partial excision of the right side of the tongue was performed under general anesthesia.

After surgery, swollen lymph nodes were observed upon diagnostic imaging inspection, and the entire lymph node on the right side of the neck was then excised under general anesthesia.

Histopathological examination

The original tumor of the tongue and metastatic lymph node were fixed with a 10% buffered neutral formalin solution at 4 °C for approximately 7 days. After dehydration with graded ethanol, the tissues were dipped in xylene and embedded in paraffin. Next, 5- μ m sections were prepared for hematoxylin and eosin (HE) staining or immunohistochemical staining.

Establishment of the cell line

The metastatic lymph nodes from the neck of the patient with lingual cancer were resected, cut into small pieces with razor blades and dissociated with 0.1% trypsin-0.02% ethylenediaminetetra-acetic acid (EDTA)/phosphate-buffered saline (-) at 37 °C for 30 min. After adding a little fetal bovine serum, the fragments were further dissociated into single cells by vigorous pipetting. The dissociated cells and small fragments were centrifuged at 1,500 rpm for 5 min at room temperature. The precipitate was resuspended in growth medium (GM) and cultured in 60-mm dishes in a CO₂ incubator (4.7% CO₂, 95.3% air) at 37 °C. The GM used in this study contained: DMEM/F-12 supplemented with 15% fetal bovine serum (Sigma, Lot no. 12E261), 100 μ M of glutaMAX, 0.1% modified Eagle medium-non-essential amino acids, 50 U/ml of penicillin, 50 μ g/ml of streptomycin, and 0.25 μ g/ml of Fungizone (all purchased from Thermo Fisher Scientific Inc.). The number of floating cells and fibroblastic cells gradually decreased over the course of the culture, resulting in establishment of the hZK-1 cell line. After the cells reached confluency, they were split and inoculated at a ratio of 1:3 to 1:5 into fresh GM. The GM was changed twice a week.

Cell growth

The hZK-1 cells were seeded at a density of 1×10^4 cells/35-mm dish and were cultured

1
2
3 at 37 °C for 12 days. In order to draw the growth curve of the cell line, the number of
4 cells in five dishes was counted every 2 days. The doubling time and saturation density
5 were obtained from the growth curves.
6
7

8 9 Chromosomal analysis

10 The cells (passage 20) were treated with 1×10^{-7} M colcemid (Thermo Fisher Scientific
11 Inc.) for 4 h at 37 °C, placed in a hypotonic 0.075 M KCl solution for 20 min at 37 °C,
12 and then fixed with a methanol-acetic acid (3:1) solution at 0 °C for 10 min. After
13 fixation, the cells were stained with a 4% Giemsa solution. In addition, cells at the
14 metaphase stage were treated with a 0.1% trypsin solution for 15 s at room temperature,
15 stained with a 3% Giemsa solution (pH 6.8), and analyzed for G-band karyotyping.
16 Histograms of chromosome number distribution were prepared from the values
17 obtained from more than 50 metaphases.
18
19
20
21
22
23

24 25 Cell cross-contamination check

26 We carried out DNA profiling to confirm that there was no cross-contamination between
27 the hZK-1 and the Nialym cell line⁸). Genomic DNA was isolated from these cell lines
28 using the QIAamp DNA Mini Kit (Qiagen, Hilden, Germany) according to the
29 manufacturer's instructions. For the genetic analysis, the AmpFISTR® Identifiler®
30 PCR Amplification Kit (Applied Biosystems, Foster City, CA, USA) was used according
31 to the manufacturer's instructions, using approximately 1 ng of DNA template in a total
32 PCR volume of 25 µL. The amplified DNA markers were: D8S1179, D21S11, D7S820,
33 CSF1PO, D3S1358, TH01, D13S317, D16S539, D2S1338, vWA, TPOX, D18S51,
34 Amelogenin, D5S818 and FGA. A negative extraction and amplification control was
35 used instead of the cell lines to check for DNA contamination. The DNA of each cell line
36 and of the mixed cell lines was extracted and amplified in duplicate. A 1.5 µL aliquot of
37 the amplified PCR product was combined with 24.5 µL of Hi-Di Formamide and 0.5 µL
38 of the GeneScan 500 LIZ™ size standard. Electrophoresis was performed on an ABI
39 PRISM 310 Genetic Analyzer (Applied Biosystems). The results were analyzed using
40 GeneMapper ID v3.2 software (Applied Biosystems). The analytical threshold was set at
41 150 relative fluorescence units (RFU) in cell lines hZK-1 and Nialym. The minimum
42 peak height threshold was set at 50 RFU in the mixed cell lines. The random match
43 probability was calculated using the allele frequency in the Japanese population.
44
45
46
47
48
49
50
51
52
53
54
55

56 57 Electron microscopy

58 Cultured cells in 35-mm dishes were rinsed with Hanks' solution, and fixed with a
59
60
61
62
63
64
65

1
2
3 2.5% glutaraldehyde solution in 0.1 M phosphate buffer for 30 min. Then, the cells were
4 rinsed with the same buffer and post-fixed with 1% osmium tetroxide. After dehydration
5 with graded ethanol, followed by propylene oxide, the cells were embedded in Epon.
6 Ultrathin sections were prepared using a Leica Ultracut UCT microtome (Leica.); they
7 were stained with uranyl acetate and lead citrate, and observed with a Hitachi H-7500
8 transmission electron microscope (Hitachi, Tokyo, Japan).
9
10
11
12

13 Immunocytochemistry of hZK-1 cells

14
15 Immunocytochemical studies using antibodies against cytokeratin (CK) 17 (1:20, E3;
16 Dako, Glostrup, Denmark), CK13 (1:400, DE-K13; Dako), Ki67 (1:100, ab15580; Abcam,
17 Cambridge, UK) and p53 (1:100, PAb 240; Abcam) were performed. For
18 immunocytochemistry, the hZK-1 cells were fixed with absolute methanol (Wako Pure
19 Chemical Industries, Osaka, Japan) at 30 °C for 10 min, and then incubated in Blocking
20 One Histo (Nacalai Tesque, Japan) for 30 min at room temperature. The cultures were
21 incubated with the primary antibodies at 4 °C overnight. The samples were then
22 incubated with the following secondary antibodies for 30 min in the dark at room
23 temperature: Alexa Fluor 488-conjugated goat anti-mouse immunoglobulin G (IgG) or
24 Alexa Fluor 488-conjugated donkey anti-rabbit IgG (all diluted 1:1000; Invitrogen). The
25 nuclei were stained using VECTASHIELD® HardSet™ Mounting Medium with DAPI
26 (Vector Laboratories). Images were observed under a confocal laser scanning microscope
27 (LSM-510; Carl Zeiss, Jena, Germany).
28
29
30
31
32
33
34
35
36

37 Reverse transcription-polymerase chain reaction (RT-PCR)

38
39 Total RNA was isolated from cultured cells using an RNeasy Mini kit (Qiagen, Hilden,
40 Germany). Using 1 µg of total RNA, cDNA was synthesized with a High-Capacity cDNA
41 Reverse Transcription kit (Applied Biosystems, Carlsbad, CA, USA). Amplification was
42 performed using a PCR Supermix Platinum kit (Invitrogen, USA), a Veriti™ 96-well
43 thermal cycler, and the primers and annealing temperatures for each gene that are
44 shown in Supplementary Table 1¹⁸. The PCR products were analyzed by electrophoresis
45 on a 2% (w/v) agarose gel and stained with ethidium bromide.
46
47
48
49
50

51 PCR for HPV.

52
53 DNA was extracted from hZK-1 cells using the DNeasy Blood and Tissue Kit (QIAGEN,
54 Hilden, Germany) according to the manufacturer's instructions.

55
56 DNA sequences encoding HPV16 and HPV18 were amplified by PCR using the
57 Platinum PCR superMix (Life Technologies Corporation, Carlsbad, CA USA) and the
58
59
60
61
62
63
64
65

1
2
3 primers and PCR conditions for each gene that are shown in Supplementary Table 2.
4 The PCR products were electrophoresed in 2% agarose gels. The HeLa and TC-YIK ¹⁹⁾
5 cell lines were used as positive controls for HPV18 and HPV16, respectively.
6
7

8 9 Transplantation

10 The hZK-1 cells (1×10^7 cells/mouse in 0.5 ml of Hanks' solution) were subcutaneously
11 injected into the dorsal neck skin of three SCID mice (male, 5 weeks old; Clea, Tokyo,
12 Japan) using a 23-gauge needle. Five weeks after the transplantation, we checked a
13 presence of formation of a tumor.
14
15
16

17 18 Assay of HIF-1 α expression and VEGF secretion

19 Cellular HIF-1 α expression and amount of VEGF secretion were measured using an
20 enzyme-linked immunosorbent assay (ELISA).
21

22
23 Nearly confluent hZK-1 cells (1×10^6 cells, at the 10th, 20th, and 30th passage) were
24 incubated in GM for 4 hours under normoxic (air) or hypoxic (5% O₂) conditions at 37 °C.
25 The cells were then fixed and processed according to the assay protocols described below.
26 The amount of cellular HIF-1 α was analyzed using the HIF-1 Alpha cell based ELISA
27 kit (CBA-281), (Cell Biolabs, Inc. San Diego, CA, USA) and the amount of VEGF in the
28 conditioned medium was analyzed using a VEGF ELISA kit (DVE00; R&D Systems,
29 Minneapolis, MN, USA). Briefly, the HIF-1 Alpha cell based ELISA kit is an
30 immunoassay that was developed for rapid detection of HIF-1 α in fixed cells. Cells on a
31 microplate are stimulated for HIF-1 α stabilization, fixed, permeabilized, and then
32 neutralized in the well. HIF-1 α is then detected with an anti-HIF-1 α antibody followed
33 by an HRP conjugated secondary antibody. In addition, in order to confirm inhibition of
34 VEGF secretion by YC-1, which is an inhibitor of HIF-1 α , hZK-1 cells (1×10^6 cells, at
35 the 10th, 20th, and 30th passage) were treated with 80 μ mol/L YC-1 in the presence of 0.5
36 mmol/L cobalt chloride at 37 °C for 4 hours. The amount of VEGF in the conditioned
37 medium was then assayed using the VEGF ELISA kit.
38
39
40
41
42
43
44
45
46
47

48 49 Anticancer drug susceptibility tests of in vitro cultured hZK-1 cells

50 Anticancer drug (cisplatin (CDDP), docetaxel (TXT), 5-fluorouracil (5-FU) and a
51 mixture of the 3 agents) susceptibility tests were carried out using an oxygen electrode
52 apparatus (Aloka Co LTD., Dox-24, Tokyo, Japan) ²⁰⁾. hZK-1 cell suspensions were
53 centrifuged at 430 \times g for 5 min. Pellets were resuspended with 2 ml of HEPES-GM
54 containing one of the anticancer drugs (CDDP, 0.2 μ g/ ml or 1 μ g/ ml; TXT, 1 μ g/ ml or 5
55 μ g/ ml; 5-FU, 1 μ g/ ml or 5 μ g/ ml). Cell-drug suspensions were then transferred to the
56
57
58
59
60
61
62
63
64
65

1
2 oxygen electrode meter at 37 °C and dissolved oxygen in the cell-drug medium was
3 measured for 16 h (2×10^6 cells/tube). Analysis of susceptibility to anticancer drugs was
4 carried out using the method of Uesu and Ishikawa ²¹⁾.
5
6
7

8 Results

9 Histopathological diagnosis

10 The histopathological diagnosis of the original tumor was moderately or
11 well-differentiated squamous cell carcinoma of the tongue (Fig. 1a). Abundant blood
12 vessels were observed in HE-stained tumor tissue (Fig. 1b). HE staining of the
13 metastatic lymph node is shown in Fig. 1c. A blood vessel that had developed within the
14 tumor tissue in the lymph node could be seen.
15
16
17
18
19

20 Establishment of the hZK-1 cell line

21 The hZK-1 cell line was established from the metastatic foci of the lymph node from
22 the neck of the patient with lingual cancer. Epithelial cells and fibroblastic cells were
23 intermingled in the primary culture (Fig. 2a). Over the course of serial passages, the
24 number of fibroblastic cells gradually decreased, and the hZK-1 cell line was
25 established.
26
27
28
29
30

31 Morphology of the hZK-1 cells

32 Deformity of the hZK-1 cells was common. The cells displayed a jigsaw puzzle-like
33 arrangement. Moreover, they were observed to pile up in some places. The size of the
34 cells varied, and the nuclear membranes were pseudomorphic. The nucleoli were clear
35 and the cytoplasm had a bright appearance (Fig. 2b).
36
37
38
39
40

41 The growth characteristics of the hZK-1 cell line

42 The doubling time of the hZK-1 cells was approximately 36, 33 and 29 h, and the
43 saturation density was 0.21×10^4 , 0.23×10^4 and 0.25×10^4 cells/cm² for cells at the 10th,
44 20th and 30th passage, respectively.
45
46
47
48
49

50 Chromosomal analysis and distribution

51 The results of chromosomal analysis of the hZK-1 cells are shown in Supplementary
52 Fig. 1. The cell line was shown to be triploid, with a chromosomal distribution of 75 to
53 80. The modal number was 76 to 78. There were many (21~27) marker chromosomes.
54 The karyotype was determined to be 76~79(3n), -X[10], add(X)(q11)x2[10],
55 add(1)(p11)[10], add(1)(q11)[10], del(1)(p11)[8], add(2)(q35)[7],
56
57
58
59
60
61
62
63
64
65

1
2
3 der(2)add(2)(p11)add(2)(q35)[3], der(2;12)(q10;q10)del(2)(q35)[8],
4 der(2;12)(q10;q10)add(12)(q24)del(2)(q35)[9], add(3)(p21)[9], add(3)(p25~26)[10],
5 der(3)t(3;12)(p13;q13)add(3)(q27)[10], -4[10],add(4)(q21)x2[10], -5[10],
6 add(5)(p11)x2[10], -6[10], -6[9], del(6)(q13)[10], -7[10]add(7)(p11)[10],
7 der(7)add(7)(p11)add(7)(q32)[9]-8[10], add(8)(q22)[10], add(8)(q22)[10], -9[9],
8 del(9)(p12)x2[10]+10[5], -11[10], add(11)(p11)[9], add(11)(q13)[9], -12[10], -12[10],
9 add(12)(q27)[8], -13[7], add(13)(p11)[9], -14[10], add(14)(q22)[10]add(14)(q22)[10], -15[6],
10 add(15)(p11)x2[10], add(15)[4], -16[10], -16[3], -17[10], add(17)(p11)[7]-18[9], -19[6],
11 +20[9], +21[3], -22[4], +21~27mar.
12
13
14
15
16
17

18 Cell cross-contamination check

19 The DNA profile obtained for the hZK-1 cell line did not match that of the Nialym cell
20 line, which proved that there was no cross contamination between these cell lines
21 (figure not shown).
22
23
24
25

26 Electron micrographic analysis of the hZK-1 cells.

27 Electron microscopic observations revealed that the nuclear membranes were
28 pseudomorphic, and that the cells had a clear and large nuclear body and many kinds of
29 intracellular organelles. Although little development of rough-ER (r-ER) was seen,
30 concentric r-ER was occasionally observed (Supplementary Fig. 2). Moreover,
31 desmosomes and many microvilli were present (Fig. 3). There was a small number of
32 glycogen granules (figure not shown). Lysosomes, lipid droplets, free ribosomes, and the
33 Golgi apparatus were also observed in the hZK-1 cells. Secretory-like granules were
34 observed around the Golgi apparatus (Supplementary Fig. 2). There were no virus-like
35 particles. Tonofilaments, which are one of the features of epithelial cells, were poorly
36 developed.
37
38
39
40
41
42
43
44

45 Immunofluorescence observations

46 The hZK-1 cells stained positive for CK17, Ki67 and p53, but were negative for CK13
47 (Fig. 4a, b, c, d).
48
49
50

51 Reverse transcription-polymerase chain reaction (RT-PCR)

52 The mRNA expression of CK17, Ki67, and p53 was elevated (Supplementary Fig. 3).
53
54
55

56 PCR for Human papillomavirus (HPV)

57 Expression of HPV16 and HPV18 in hZK-1 cells and in the HPV-positive control cell
58
59
60
61
62
63
64
65

1
2 lines TC-YIK or HeLa, was tested using PCR with primers specific for HPV16 and
3 HPV18 (Supplementary Table 2). This PCR analysis showed that hZK-1 cells were
4 negative for HPV infection (Supplementary Fig. 4).
5
6

7 8 9 Transplantation of the hZK-1 cells into SCID mice

10 None of the subcutaneous injections of hZK-1 cells into SCID mice resulted in a
11 successful transplant.
12
13

14 15 Analysis of VEGF secretion and HIF-1 α expression in hZK-1 cells

16 hZK-1 cells at the 10th, 20th and 30th passages secreted VEGF in 3-day cultures. The
17 amounts of VEGF secreted are shown in Fig. 5a. The amount of VEGF secreted by
18 hZK-1 cells was increased under hypoxic conditions compared to that under normoxic
19 conditions. In the YC-1 addition group, a decrease in the amount of VEGF secretion was
20 observed under both hypoxic and normoxic conditions in comparison with the group to
21 which YC-1 was not added. However, the differences in the amount of VEGF secreted by
22 the YC-1 treated groups under the different oxygen conditions were small.
23
24

25 The amounts of cellular HIF-1 α under the different conditions are shown in Fig. 5b.
26 The amount of HIF-1 α was greatly increased under the hypoxic condition compared to
27 that under the normoxic condition.
28
29

30 31 32 Anticancer drug susceptibility testing of hZK-1 cells

33 Susceptibility testing for anticancer drugs revealed that hZK-1 cells were not sensitive
34 to 0.2 or 1 μ g/ml CDDP, 1 or 5 μ g/ml TXT, 1 or 5 μ g/ml 5-FU, or a mixture of the 3 agents
35 at low or high concentrations (Supplementary Fig. 5). Thus, hZK-1 cells were not
36 sensitive to any of these anticancer drugs.
37
38
39
40
41
42

43 44 Discussion

45 The Nialym cell line⁸⁾, which we previously established from squamous carcinoma of
46 the tongue, is composed of cells with a bright or a dark appearance under the light
47 microscope. Of note, the dark cells have many tonofilaments. However, the hZK-1 cell
48 line is composed of only bright cell, and tonofilaments are not well developed.
49 Furthermore, since the hZK-1 cell line and the Nialym cell line were both derived from
50 OSCC of the tongue, we checked the presence of cross contamination between these two
51 cell lines by AmpFLSTR[®] Identifiler[®] PCR Amplification. Cross contamination between
52 the two cell lines was not found.
53
54

55 OSCC is characterized by a high degree of local invasiveness to surrounding tissues,
56
57
58
59
60
61
62
63
64
65

1
2
3 which can be a cause of treatment failure. One of the difficulties in studying the
4 metastasis of human OSCC is the lack of an appropriate animal model and OSCC cell
5 lines²²⁾. Most existing OSCC cell lines have been established from metastatic lymph
6 nodes^{23, 24)} as in the present study.
7
8

9 Since the original cancer had an abundance of blood vessels, it was assumed that the
10 cancer cells were producing an angiogenic factor. We therefore assayed the production of
11 VEGF (a known angiogenic factor) by the cancer cells. VEGF is a major regulator of
12 both physiological and pathological angiogenesis^{10, 11)}. The mechanism of cancer cell
13 metastasis is not yet clear. However, after the migration of cancer cells into normal
14 tissue, the cancer cells are regarded to be in hypoxic conditions. We therefore considered
15 that cancer cells in a metastatic focus would be in hypoxic conditions and may produce
16 HIF-1 α , which would then enhance the production of VEGF. We therefore evaluated the
17 quantity of HIF-1 α and VEGF produced by hZK-1 cells. HIF-1 α plays a critical role in
18 angiogenesis by activating the transcription of genes that encode pro-angiogenic growth
19 factors, including VEGF, basic fibroblast growth factor (bFGF), angiopoietin-1 and -2,
20 placental growth factor, and platelet-derived growth factor-B^{14,25)}. The hZK-1 cells could
21 not be successfully transplanted into SCID mice, even though the cells secreted a
22 moderate level of VEGF. The mechanisms behind graft rejection and angiogenesis
23 remain unknown. It has been recently suggested that the VEGF-C/VEGFR-3 axis may
24 be associated with lymph node metastasis of tongue squamous cell carcinoma through
25 lymphangiogenesis²⁴⁾. High expression of VEGF-C in the primary tumor may be a good
26 determinant for detection of occult tumor cells in the lymph nodes of OSCC cases²⁶⁾. It is
27 therefore important to carry out research for the development of anti-tumor drugs such
28 as VEGF-depleting and VEGF receptor-inhibiting drugs²⁷⁾. HIF-1 α and CD44
29 immunohistochemical detection could potentially serve as a prognostic tool in therapy
30 selection for early-stage OSCC²⁸⁾. We observed that inhibition of HIF-1 α by YC-1
31 partially inhibited VEGF expression in hZK-1 cells. The hZK-1 cells were shown to be
32 triploid in the karyotype analysis, and the large number of marker chromosomes
33 suggests that the grade of malignancy of these cells was high. HPV is one of the most
34 common sexually transmitted infections worldwide. In 2007, HPV-16 was recognized as
35 a risk factor by the International Agency for Research on Cancer, for oropharyngeal
36 squamous cell carcinoma (OSCC), where tonsillar and base of tongue cancer dominate.
37 Over the past 20-40 years, the incidence of HPV-positive tonsillar and base of tongue
38 cancer has risen in many western countries, and >70% of these cancers are in men²⁹⁾.
39 We did not detect HPV in the hZK-1 cells, indicating that the immortalization of these
40 cells was not caused by virus transfection. hZK-1 cells were not sensitive to any of the
41
42
43
44
45
46
47
48
49
50
51
52
53
54
55
56
57
58
59
60
61
62
63
64
65

1
2 anticancer drugs that we tested.

3
4 These hZK-1 cells may be a very useful cell line for the development of chemotherapies
5 or immune therapies for HPV-independent OSCCs.
6

7
8
9 **Acknowledgements**

10 We thank Drs. Akihiro Ohyama, Junko Toyomura, Minako Suzuki, Miyuki Kawakami,
11 and Taka Nakahara for helpful discussions.
12
13

14
15 **Author Disclosure Statement**

16 No competing financial interests exist.
17
18

19
20 **Ethical approval**

21 All procedures were approved by the ethics committee of the School of Life Dentistry,
22 Nippon Dental University, Japan (approval number: NDU-T2013-04).
23
24

25
26 **References**

- 27
28 1. Massano J, Regateiro F, Januario G, Ferreira A. Oral squamous cell carcinoma:
29 review of prognostic and predictive factors. *Oral Surg Oral Med Oral Pathol Oral Radiol*
30 *Endod* (2006) 102: 67-76.
31
32 2. Som PM. Detection of metastasis in cervical lymph nodes: CT and MRI criteria and
33 differential diagnosis. *Am J Radiol* (1992) 158: 961-9.
34
35 3. Yasui A, Okada Y, Mataga I, Katagiri M. An analysis of distant metastasis in oral
36 squamous cell carcinoma. *J Hard Tissue Biol* (2010) 19: 27-32.
37
38 4. Gioanni J, Fischel JL, Lambert JC, et al. Two new human tumor cell lines derived
39 from squamous cell carcinomas of the tongue: establishment, characterization and
40 response to cytotoxic treatment. *Eur J Cancer Clin Oncol* (1988) 24: 1445-55.
41
42 5. Chew EC, King WK, Hou HJ, Yam HF. Establishment and characterization of two
43 new cell lines derived from squamous cell carcinoma of the tongue in Chinese patients.
44 *Anticancer Res* (1992) 12: 1627-34.
45
46 6. King WWK, Lam PK, Huang DWSP, Liew CT, Li AKC. Establishment and
47 characterization of a human cell line from a squamous carcinoma of the tongue. *Clin*
48 *Otolaryngol* (1995) 20: 15-20.
49
50 7. Kim KM, Park EJ, Yeo YH, Cho KJ, Kim MS. Establishment of a novel HPV-negative
51 and radiosensitive head and neck squamous cell carcinoma cell line. *Head and Neck*
52 (2015) Mar 17. doi: 1002/hed.24037
53
54 8. Takahashi H, Ishikawa H, Mataga I, et al. Establishment and characterization of
55
56
57
58
59
60
61
62
63
64
65

1
2
3 human lingual squamous cell carcinoma cell lines designated Nialym derived from
4 metastatic foci of lymph node, and Nialymx derived from transplanted tumor of Nialym
5 cells. *Human Cell* (2015) 28:143-153.
6

7 9. Han J, Kioi M, Chu WS, et al. Identification of potential therapeutic targets in human
8 head and neck squamous cell carcinoma. *Head and Neck Oncol*, 2009; 1,27.
9

10 10. Koch S, Yao C, Grieb G, Prevel P, Noah EM, Steffens GCM. Enhancing angiogenesis
11 in collagen matrices by covalent incorporation of VEGF. *J Mater Sci Mater Med* 2006,
12 17: 735-41.
13
14

15 11. Nor JE, Christensen J, Mooney DJ, Polverini PJ. Vascular endothelial growth factor
16 (VEGF)-mediated angiogenesis is associated with enhanced endothelial cell survival
17 and induction of Bcl-2 expression. *Am J Pathol* 1999;154:375-84.
18

19 12. Benjamin LE, Hemo I, Keshet E. A plasticity window for blood vessel remodeling is
20 defined by pericyte coverage of the preformed endothelial network and is regulated by
21 PDGF-B and VEGF. *Development* 1998; 125:1591-8.
22
23

24 13. Haspel HC, Scicli GM, MaMahon G, Scicli GM. Inhibition of vascular endothelial
25 growth factor-associated tyrosine kinase activity with SU5416 blocks sprouting in the
26 microvascular endothelial cell spheroid model of angiogenesis. *Microvasc Res* 2002;63:
27 304-15.
28
29
30

31 14. Forsythe JA, Jiang BH, Lyer NV, et al. Activation of vascular endothelial growth
32 factor gene transcription by hypoxia-inducible factor 1. *Mol Cell Biol* 1996; 16: 4604-13.
33

34 15. Wong GL, Jiang BH, Rue EA, Semenza GL. Hypoxia-inducible factor 1 is a
35 basic-helix-loop-helix-PAS heterodimer regulated by cell OXYGEN tension. *Proc Natl*
36 *Acad Sci* 1995; 92: 5510-4.
37
38

39 16. Identity crisis. *Nature*. 2009;457 (7232):935-6

40 17. Chatterjee R. Cell biology. Cases of mistaken identity. *Science*. 2007;315
41 (5814):928-31
42

43 18. Patti E, Gravitt, Cheri Peyton, Cosette Wheeler, Raymond Apple, Russell Higuchi,
44 Keerti V. Shah. Reproducibility of HPV 16 and HPV 18 viral load quantitation using
45 TaqMan real-time PCR assays. *J Virol Methods*. 2003 Sep;112(1-2):23-33
46

47 19. Ichimura H, Yamasaki M, Tamura, et al. Establishment and Characterization of a
48 New Cell Line TC-YIK Originating From Argyrophil Small Cell Carcinoma of the
49 Uterine Cervix Integrating HPV16 DNA. *Cancer*. 1991 May 1;67(9):2327-32.
50

51 20. Amano Y, Okumura C, Yoshida M et al. Measuring respiration of cultured cell with
52 oxygen electrode as a metabolic indicator for drug screening. *Hum Cell* 1999; 12: 3-10.
53

54 21. Uesu K, Ishikawa H. Analysis of an in vitro susceptibility test of anticancer drugs
55 using new types of oxygen electrodes. *Bull Edu Res Nihon Univ Sch Dent Matsudo*.
56
57
58
59
60
61
62
63
64
65

1
2
3 2005;7:7-21.

4 22. Sun R, Zhang JG, Guo CB. Establishment of cervical lymph node metastasis model
5 of squamous cell carcinoma in the oral cavity in mice. *Chinese Medical J* (2008) 121:
6 1891-5.

7
8 23. Monose F, Araida T, Negishi A, Ichijo S, Sasaki S. Variant sublines with different
9 metastatic potentials selected in nude mice from human oral squamous cell carcinomas.
10 *J Oral Pathol Med* (1989) 18: 391-5.

11
12 24. Yokoi T, Yamaguchi A, Odajima T, Furukawa K. Establishment and characterization
13 of a human cell line derived from a squamous cell carcinoma of the tongue. *Tumor Res*
14 (1988) 23: 43-57.

15
16 25. Manalo DJ, Rowan A, Lavoie T. et al. Transcriptional regulation of vascular
17 endothelial cell responses to hypoxia. *Blood* 2005; 105: 659-69.

18
19 26. Dunkel J, Vaittinen S, Grénman R, et al. Prognostic markers in stage I oral cavity
20 squamous cell carcinoma. 2013, *Laryngoscope* 123:2435-43.

21
22 27. Kazakydasan S, Rahman ZA, Ismail SM, et al. Prognostic significance of VEGF-C in
23 predicting micrometastasis and isolated tumour cells in NO oral squamous cell
24 carcinoma. *J Oral Pathology & Medicine*.2016.doi:10.1111/jop.12476.

25
26 28. Bozec A, Gros FX, Penault-Llorca F, et al. Vertical VEGF targeting: a combination of
27 ligand blockade with receptor tyrosine kinase inhibition. *European J Cancer* 2008, 44:
28 1922-30.

29
30 29. Bucchi D, Stracci F, Buonoraet N, et al. Human papilloma virus and gastrointestinal
31 cancer: a review. *World J. of Gastroenterology* 2016, September 7; 22(33): 7415-7430.
32
33
34
35
36
37
38
39
40
41
42
43
44
45
46
47
48
49
50
51
52
53
54
55
56
57
58
59
60
61
62
63
64
65

1
2
3 **Figure Legends**
4

5
6 **Fig. 1**

7 The pathological diagnosis of the original tumor is moderate-to-well differentiated
8 squamous cell carcinoma. (a) Low magnification, and (b) High magnification of a HE-
9 stained tumor section. Stratified squamous epithelium is indicated (arrow in a). Scale
10 bar: 200 μm . (c) HE staining of the histopathological aspect of the metastatic focus of the
11 lymph node. Note a blood vessel that is developing within the tumor tissue (arrows).
12 Pleomorphic tumor cells form colonies that are scattered throughout the lymph node.
13 Scale bar: 100 μm .
14
15
16
17
18
19

20 **Fig. 2**

21 (a) Phase contrast micrograph of the primary culture. In addition to epithelial cells,
22 skeletal muscle-like cells (arrows), fibroblastic cells and multi-nucleated cells (arrow
23 heads) can also be seen. (b) Phase contrast micrograph of hZK-1 cells at the 30th passage.
24 Cells in a jigsaw puzzle-like arrangement are observed. Some cells have long projections
25 and touch other cells with these projections. Many mitotic figures can be seen. Scale bar:
26 100 μm .
27
28
29
30
31

32 **Fig. 3**

33 Transmission electron micrographs of hZK-1 cells.

34 Many nuclear membranes were almost smooth in appearance. Interdigitation via
35 microvilli was observed between the cells. Many free ribosomes were observed. Moreover,
36 a small number of desmosomes (arrows) were seen. High magnification of the
37 desmosomes is shown in the upper right corner. Scale bar: 2 μm
38
39
40
41
42

43 **Fig. 4**

44 Immunocytochemical analysis of hZK-1 cells. Fluorescence immunostaining of hZK-1
45 cells for CK-17 (a), CK-13 (b), Ki67 (c) and p53 (d). Nuclei were co-stained with DAPI
46 (blue). hZK-1 cells were positive for CK-17, Ki67 and p53, but were negative for CK-13.
47 Scale bar: 50 μm .
48
49
50
51
52

53 **Fig. 5**

54 (a) Amounts of VEGF in the conditioned media of hZK-1 cells under different oxygen
55 conditions and in the presence and absence of YC-1. Data are presented as the mean \pm
56 S.D. (b) Amounts of HIF-1 α in the hZK-1 cells under different oxygen conditions. Data
57
58
59
60
61
62
63
64
65

1
2
3
4
5
6
7
8
9
10
11
12
13
14
15
16
17
18
19
20
21
22
23
24
25
26
27
28
29
30
31
32
33
34
35
36
37
38
39
40
41
42
43
44
45
46
47
48
49
50
51
52
53
54
55
56
57
58
59
60
61
62
63
64
65

are presented as the mean \pm S.D.

Figure 1

Fig.1

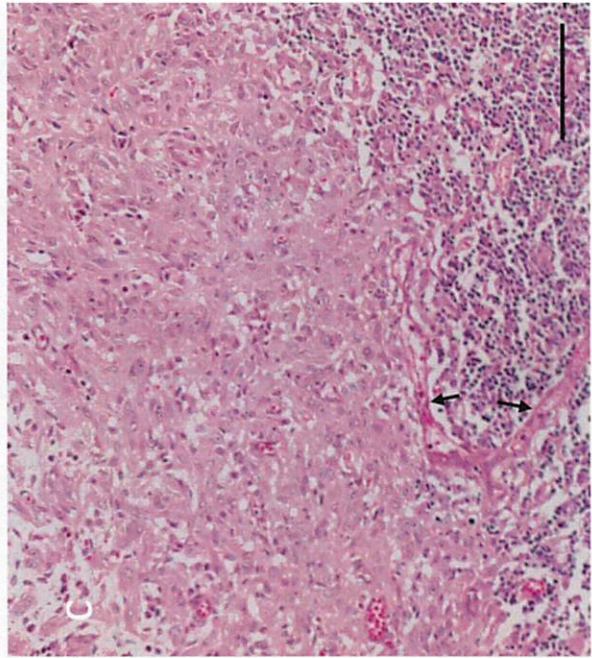
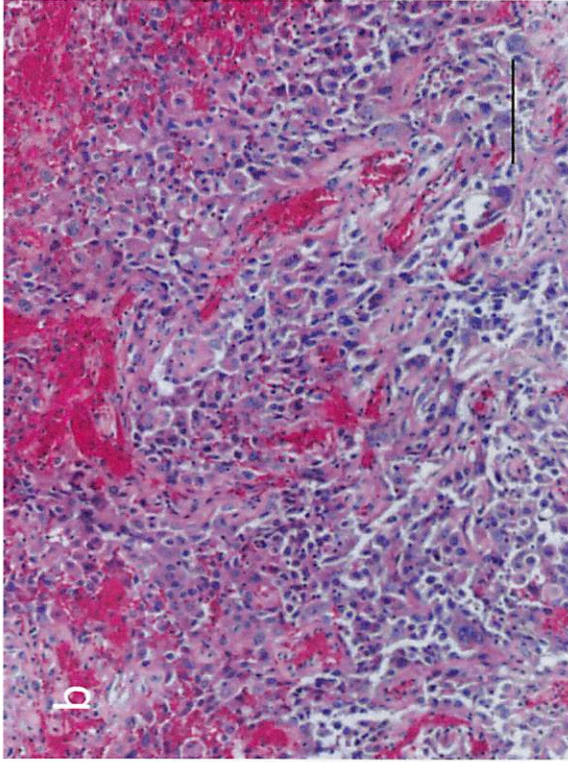
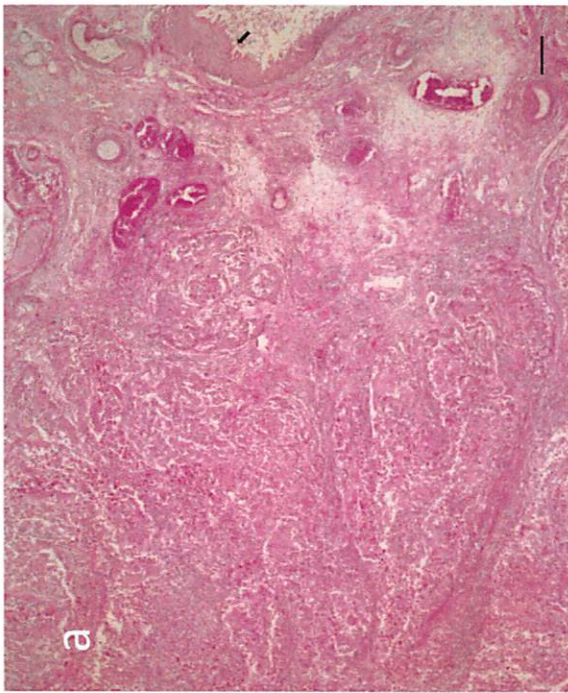


Figure 1

Figure 2

Fig.2 a

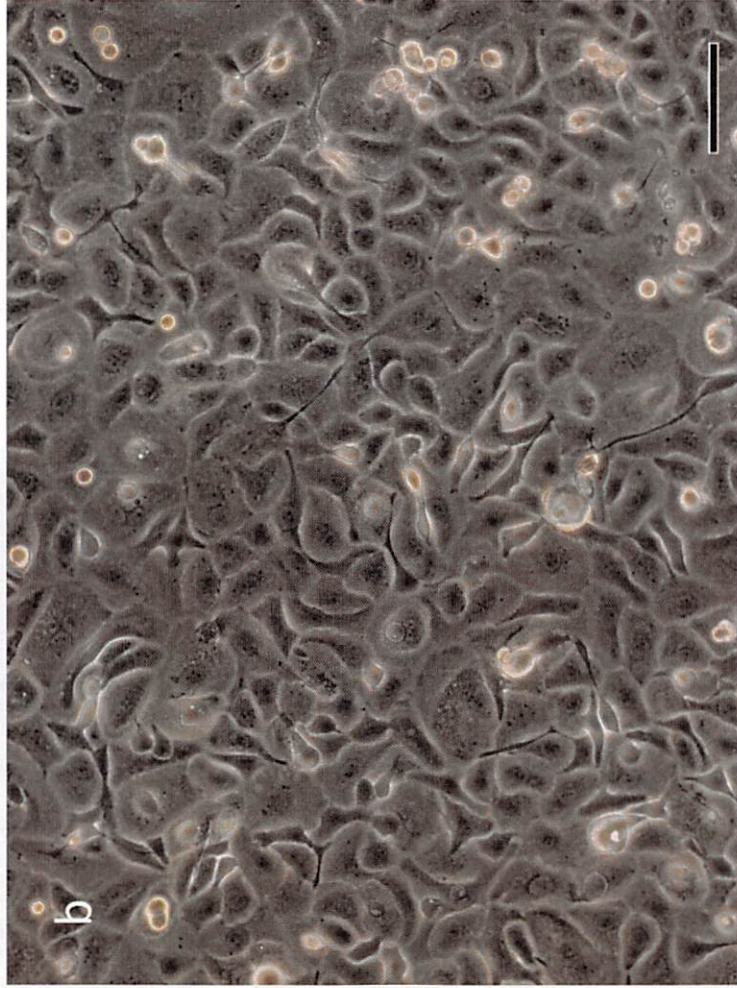


Figure 3

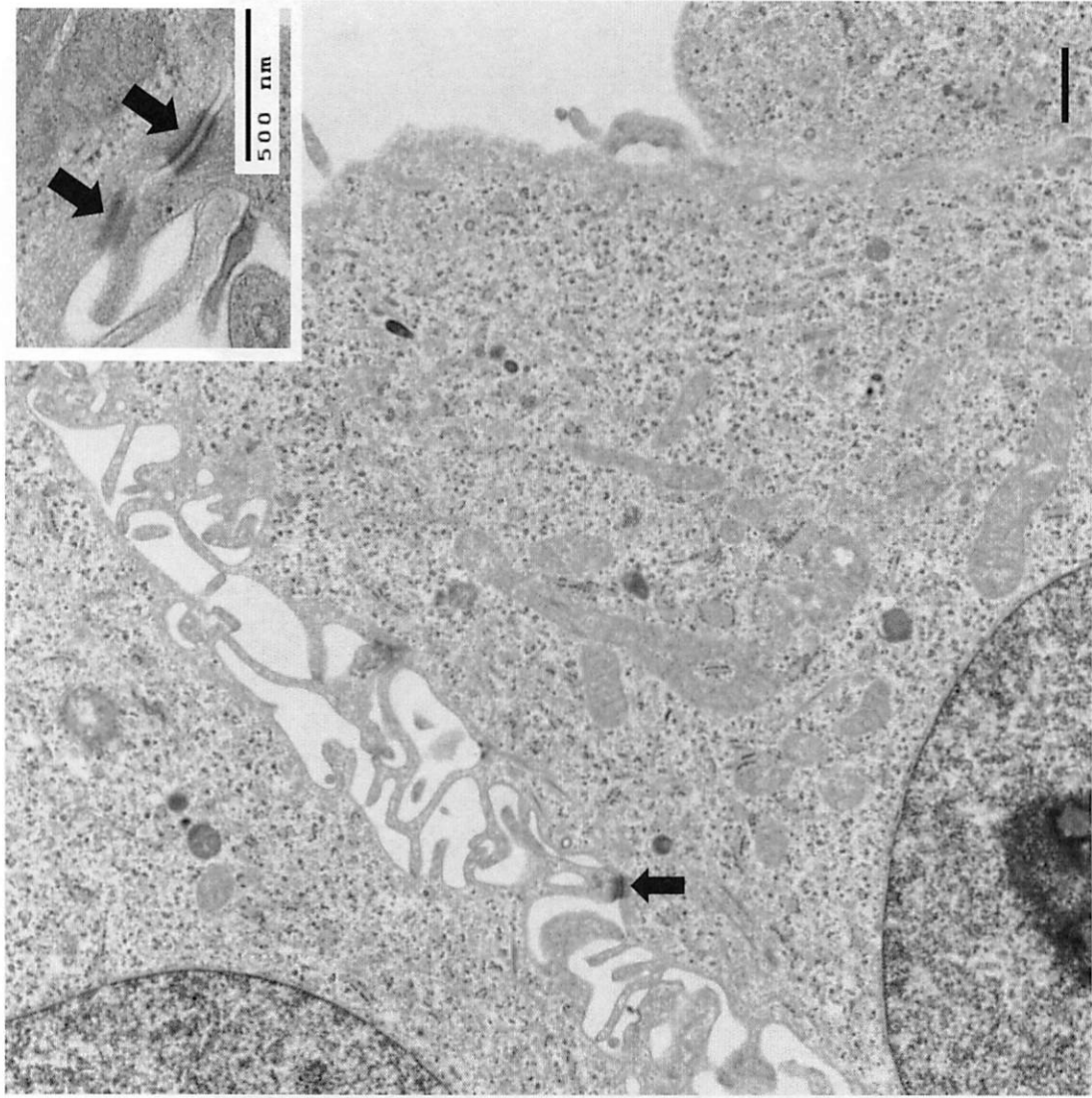


Fig. 3

Figure 4

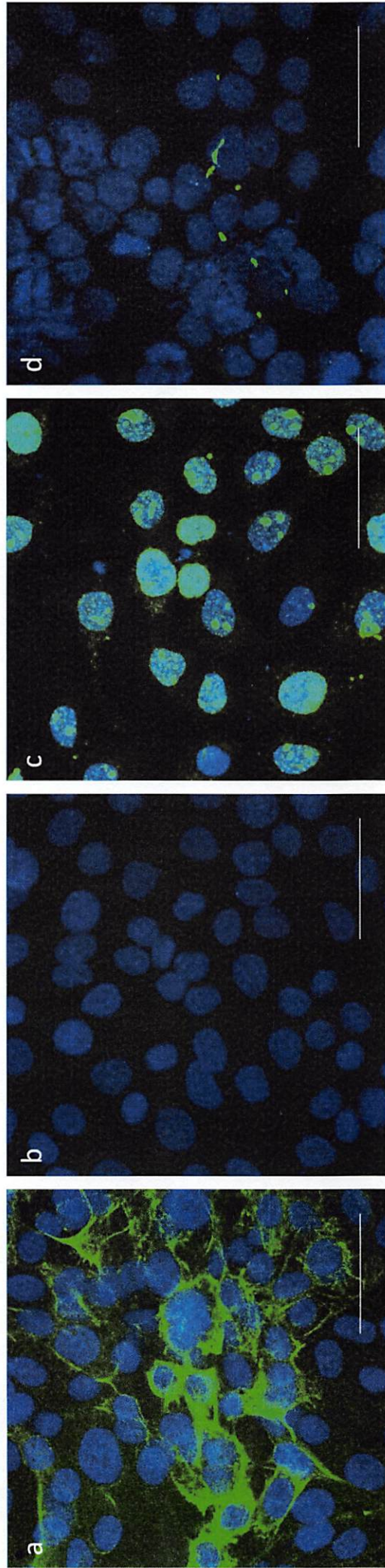


Fig.4

Figure 5

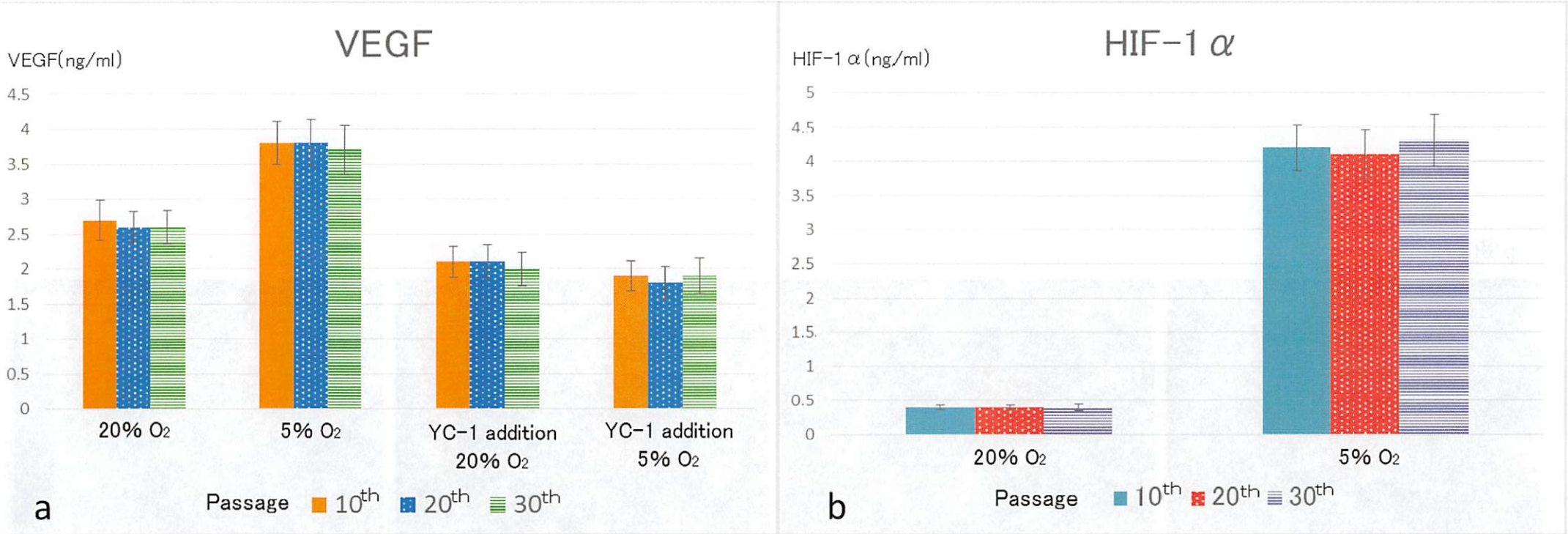


Fig.5